

Holographic Tensor Networks as Tessellations of Geometry

Qiang Wen^{a,*}, Mingshuai Xu^{a,†} and Haocheng Zhong^{a,‡}

^a*Shing-Tung Yau Center and School of Physics, Southeast University, Nanjing 210096, China*

Holographic tensor networks serve as toy models for the Anti-de Sitter/Conformal Field Theory (AdS/CFT) correspondence, capturing many of its essential features in a concrete manner. However, existing holographic tensor network models remain far from a complete theory of quantum gravity. A key obstacle is their discrete structure, which only approximates the semi-classical geometry of gravity in a qualitative sense. In [1], it was shown that a network of partial-entanglement-entropy (PEE) threads, which are bulk geodesics with a specific density distribution, generates a perfect tessellation of AdS space. Moreover, such PEE-network tessellations can be constructed for more general geometries using the Crofton formula. In this paper, we assign a quantum state to each vertex in the PEE network and develop two holographic tensor network models: the factorized PEE tensor network, which takes the form of a tensor product of EPR pairs, and the random PEE tensor network. In both models we reproduce the exact Ryu–Takayanagi formula by showing that the minimal number of cuts along a homologous surface in the network exactly computes the area of this surface.

Introduction— The Anti-de Sitter/Conformal Field Theory (AdS/CFT) correspondence [2–4], also known as the holographic principle, is a profound framework in theoretical physics that establishes an equivalence between a gravitational theory in a higher-dimensional spacetime and a quantum field theory on its lower-dimensional boundary. It provides a non-perturbative definition of quantum gravity in AdS space in terms of a well-defined quantum field theory without gravity. Moreover, the duality has deep connections to quantum information theory. For example, concepts like entanglement wedge reconstruction (or subregion duality) [5–15] reveal how quantum information in a bulk region is encoded in the boundary theory, leading to natural error-correcting properties [14, 16–21].

The tensor network approach [22–31] provides a concrete framework to explore the structure of the AdS/CFT correspondence [32]. More explicitly, we start with a space filled with tensors representing quantum states on each site in the space, then we contract the “legs” (indices) to connect adjacent tensors thus get a tensor network, which plays the role of the background geometry. The uncontracted legs of tensors in the bulk and the boundary are regarded as the bulk and the boundary degrees of freedom respectively, and the tensor network provides a quantum-error-correcting code that encodes the bulk states into the boundary Hilbert space [14, 33]. Many toy models of tensor network to simulate the AdS/CFT correspondence have been proposed (see also [34–38] for recent interesting developments), based on different structures of the networks and different quantum states associated to the tensors. One important holographic feature for these toy models is that, the entanglement entropy is given by the minimal number of cuts along a homologous surface in the network, which matches the area of the minimal surface of the celebrated Ryu–Takayanagi (RT) formula [39–44].

Nevertheless, in most of these toy models their struc-

tures of the tensor network are usually discrete and only capture the features of the background geometry in a qualitative way. There is a big gap between number of cuts in a discrete network and the area of a surface in a smooth Riemannian manifold. Recently, a continuous network as a perfect tessellation of the background AdS geometry was constructed using the so-called partial-entanglement-entropy (PEE) threads [1, 45], which are bulk geodesics with a particular density distribution determined by the PEE structure of the boundary CFT. In such a network, the number of cuts along a surface exactly reproduces the area of this surface. In this work, we will develop two toy models of tensor network based on the PEE threads (or the PEE tensor network for short) in d -dimensional Poincaré AdS space. The first one is the factorized PEE tensor network constructed via tensor product of EPR pairs. It enjoys similar properties to the Harlow–Pastawski–Preskill–Yoshida (HaPPY) code [46] which is built from perfect tensors, and perfectly reproduces the RT formula for spherical regions in the vacuum CFT state. In the second model, following [28, 33, 37, 47–49] we associate a random state to each bulk site to build the random PEE tensor network, where we can exactly reproduce the RT formula for generic boundary regions.

The network of PEE threads— The partial entanglement entropy (PEE) [50–55] is a measure of entanglement $\mathcal{I}(A, B)$ between any two non-overlapping regions A and B featured by the key property of additivity. It can be determined by the following physical requirements [51, 56]:

1. *Additivity*: $\mathcal{I}(A, B \cup C) = \mathcal{I}(A, B) + \mathcal{I}(A, C)$;
2. *Permutation symmetry*: $\mathcal{I}(A, B) = \mathcal{I}(B, A)$;
3. *Normalization*: $\mathcal{I}(A, \bar{A}) = S_A$;
4. *Positivity*: $\mathcal{I}(A, B) > 0$;
5. *Upper bounded*: $\mathcal{I}(A, B) \leq \min\{S_A, S_B\}$;

6. $\mathcal{I}(A, B)$ should be invariant under local unitary transformations inside A or B ;
7. *Symmetry:* For any symmetry transformation \mathcal{T} under which $\mathcal{T}A = A'$ and $\mathcal{T}B = B'$, we have $\mathcal{I}(A, B) = \mathcal{I}(A', B')$.

Here the regions are all non-overlapping, $A \cup \bar{A}$ makes a pure state and S_A denotes the entanglement entropy of A . The solutions for these requirements were first studied in [41] as the mutual information that is additive in some special theories, and then the solutions are understood as the PEE in [51], which is in general not a mutual information. Later it was gradually realized that, the requirement of normalization should not be imposed for an arbitrary region. In the case of the vacuum CFT state on a plane, the solution only exists if we impose the normalization requirement to spherical regions [51]. See also [50, 51, 55–57] for other prescriptions to construct the PEE which satisfy the above requirements, and see [58–65] for related discussions on PEE.

Due to the properties of additivity and permutation symmetry, any PEE $\mathcal{I}(A, B)$ can be further decomposed into a class of PEE between two different sites \mathbf{x} and \mathbf{y} , or the two-point PEE $\mathcal{I}(\mathbf{x}, \mathbf{y})$, in the following way [45, 51]:

$$\mathcal{I}(A, B) = \int_A d\mathbf{x} \int_B d\mathbf{y} \mathcal{I}(\mathbf{x}, \mathbf{y}). \quad (1)$$

Moreover, in the vacuum CFT_d on a plane the two-point PEE can be fully determined by imposing all the above requirements for the spherical regions [1, 45], i.e.

$$\mathcal{I}(\mathbf{x}, \mathbf{y}) = \frac{c}{6} \frac{2^{(d-1)} (d-1)}{\Omega_{d-2} |\mathbf{x} - \mathbf{y}|^{2(d-1)}}, \quad (2)$$

where $\Omega_{d-2} = 2\pi^{\frac{d-1}{2}}/\Gamma(\frac{d-1}{2})$ is the area of $(d-2)$ -dimensional unit sphere.

In the context of AdS/CFT, the vacuum CFT_d state on a plane is dual to the Poincaré AdS_{d+1} space. The two-point PEE $\mathcal{I}(\mathbf{x}, \mathbf{y})$ was also proposed to have a natural holographic dual [1, 45], which is the density of the bulk geodesics connecting the boundary sites \mathbf{x} and \mathbf{y} . The bulk geodesics whose density are determined in such a way are denoted as the PEE threads. Let us set that each PEE thread gives unit contribution to the PEE, then (1) captures the number of PEE threads connecting the two boundary regions A and B . The collection of all the PEE threads forms a continuous, dense network permeating the entire time slice of the Poincaré AdS_{d+1} , which we call the PEE network (see an example of $d = 2$ in Fig.1). Remarkably, it was found that [1, 45] the PEE network is a tessellation of the static AdS space in the following sense:

- Given an arbitrary $(d-1)$ -dimensional surface Σ in a time slice of AdS_{d+1} , the density of intersections between Σ and the bulk PEE network everywhere

on Σ is given by a constant $\frac{1}{4G}$, where $G = \frac{3}{2c}$ is the Newton's constant.

Then for any bulk surface Σ , the area can be reproduced by counting the number $\mathcal{N}(\Sigma)$ of intersections between Σ and the PEE network,

$$\frac{\text{Area}(\Sigma)}{4G} = \mathcal{N}(\Sigma) = \frac{1}{2} \int_{\partial\mathcal{M}} d\mathbf{x} \int_{\partial\mathcal{M}} d\mathbf{y} \omega_{\Sigma}(\mathbf{x}, \mathbf{y}) \mathcal{I}(\mathbf{x}, \mathbf{y}). \quad (3)$$

Here \mathcal{M} is a constant time slice in the Poincaré AdS_{d+1} , while $\partial\mathcal{M}$ is the boundary where the vacuum CFT state lives, and $\omega_{\Sigma}(\mathbf{x}, \mathbf{y})$ represents of the number of intersections between Σ and the particular PEE thread connecting boundary sites \mathbf{x} and \mathbf{y} .

Furthermore, it was shown in [1] that (3) is equivalent to the so-called Crofton formula in integral geometry [66] applied on a time slice of AdS_{d+1} . To be specific, consider a d -dimensional Riemannian manifold \mathcal{M} and an arbitrary $(d-1)$ -dimensional immersed hypersurface Σ , the Crofton formula states that the area of Σ can be evaluated by counting the number of intersections between Σ and the geodesics in \mathcal{M} , which forms a space $\text{Geod}(M)$ with properly chosen measure $d\Gamma$ which is called the Kinematic measure, i.e.

$$\text{Area}(\Sigma) = \frac{1}{2} \frac{d-1}{\Omega_{d-2}} \int_{\text{Geod}(M)} \#(\Gamma \cap \Sigma) d\Gamma. \quad (4)$$

Here, the integrand $\#(\Gamma \cap \Sigma)$ represents the number of intersections between any geodesic Γ in $\text{Geod}(M)$ and Σ , and the Kinematic measure $d\Gamma$ specifies the density of geodesics in some parameter space. For the case of a time slice \mathcal{M} in the AdS_{d+1} , all the geodesics can be parameterized by its boundary endpoints (\mathbf{x}, \mathbf{y}) , and the Kinematic measure $d\Gamma$ is given by,

$$d\Gamma = \det \left(\frac{\partial^2 \ell(\mathbf{x}, \mathbf{y})}{\partial \mathbf{x} \partial \mathbf{y}} \right) d\mathbf{x} \wedge d\mathbf{y} = \frac{2^{d-1}}{|\mathbf{x} - \mathbf{y}|^{2d-2}} d\mathbf{x} \wedge d\mathbf{y}, \quad (5)$$

where $\ell(\mathbf{x}, \mathbf{y})$ is the geodesic length of the geodesic connecting \mathbf{x} and \mathbf{y} . Notably, the above Kinematic measure for AdS space is proportional to $\mathcal{I}(\mathbf{x}, \mathbf{y})$ given in (2), hence we can check that (4) exactly aligns with (3).

One profound implication of the above prescription is that, minimizing the area of a surface Σ_A homologous to any boundary region A is equivalent to minimizing the number of intersections between Σ_A (see the red line in Fig.1) and the PEE network. This further implies that we can exactly reproduce the Ryu-Takayanagi (RT) formula for holographic entanglement entropy by developing proper tensor network models where the entanglement entropy of a boundary region is captured by the minimal number of intersections between a homologous surface and the PEE network [1, 45, 64]. Briefly speaking, the RT formula for the boundary region A can be

reformulated as follows,

$$S_A = \min_{\Sigma_A} \mathcal{N}(\Sigma_A) = \min_{\Sigma_A} \frac{\text{Area}(\Sigma_A)}{4G} = \frac{\text{Area}(\gamma_A)}{4G}, \quad (6)$$

where γ_A is the famous RT surface.

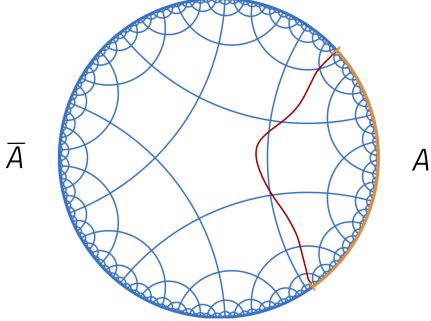


FIG. 1: Extracted from [64]. The PEE network as a tessellation of a time slice of AdS_3 . Here the blue lines represent the PEE threads, the red line is a surface Σ_A homologous to the boundary region A .

Geometric setup for bulk tensors— In a model of tensor network, a vertex at site \mathbf{z} with a set of legs corresponds to a quantum state represented by a local tensor $\mathcal{T}_{u_1 u_2 \dots}(\mathbf{z})$, where the index u_i characterizes the leg that is associated to a Hilbert space \mathcal{H}_i spanned by the basis vectors $\{|u_i\rangle\}$. Then the quantum state in the Hilbert space $\bigotimes_i \mathcal{H}_i$ settled at \mathbf{z} is defined by (assuming Einstein summation hereafter),

$$|\mathcal{T}(\mathbf{z})\rangle \equiv \mathcal{T}_{u_1 u_2 \dots}(\mathbf{z})|u_1\rangle|u_2\rangle\dots. \quad (7)$$

For simplicity, we set each of $\{\mathcal{H}_i\}$ to be the Hilbert space of a v -dimensional qudit, hence $u_i = 1, 2, \dots, v$.

Now we develop the PEE tensor networks. Consider any site \mathbf{z} in a time slice \mathcal{M} of the bulk space, for any PEE thread emanating from it to the boundary, we assign one leg that lies along this PEE thread, hence build a one-to-one correspondence between the PEE threads and the legs connecting to \mathbf{z} (see Fig.2). In the case of Poincaré AdS , any PEE thread emanating from \mathbf{z} intersects the boundary with a unique boundary site \mathbf{x} . We denote this thread as $C_{\mathbf{z}}(\mathbf{x})$, and \mathbf{x} can be used to parameterize all the threads or legs associated to \mathbf{z} . Let us denote the Hilbert space and basis vectors on each leg as $\mathcal{H}_{\mathbf{x}}$ and $|k_{\mathbf{x}}\rangle$, such that the state (7) is rewritten as

$$|\mathcal{T}(\mathbf{z})\rangle \equiv \mathcal{T}_{\mathbf{k}}(\mathbf{z}) \left(\bigotimes_{\mathbf{x} \in \text{bdy}} |k_{\mathbf{x}}\rangle \right), \quad (8)$$

where \mathbf{k} denotes a collection of indices $\{k_{\mathbf{x}}\}$, and $\{|k_{\mathbf{x}}\rangle\}$ forms an orthonormal basis for the Hilbert space associated to the index $k_{\mathbf{x}}$.

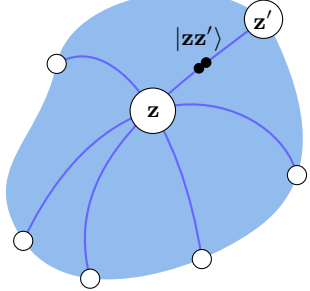


FIG. 2: A tensor state located at the bulk site \mathbf{z} (hollow white dot in the center). The legs connecting \mathbf{z} is actually continuously distributed, which can be described by a vector field as in [45]. Only six legs are exhibited, while other legs are collectively represented by the blue region. The contraction between tensors at \mathbf{z} and at adjacent site \mathbf{z}' is realized by projecting the total state into a maximally entangled state $|\mathbf{z}\mathbf{z}'\rangle$ along the PEE thread in between.

Given any adjacent site \mathbf{z}' of \mathbf{z} , there is a unique PEE thread connecting them, which picks up a pair of legs associated to \mathbf{z} and \mathbf{z}' that lie within this thread (see Fig.2). Then we contract all such pairs of legs to glue adjacent sites along the PEE threads, and finally get a quantum state $|\Psi\rangle$ for the boundary open (uncontracted) legs,

$$|\Psi\rangle = \left(\bigotimes_{\mathbf{z}, \mathbf{z}' \in \mathcal{M}} \langle \mathbf{z} \mathbf{z}' | \right) \left(\bigotimes_{\mathbf{z} \in \mathcal{M}} |\mathcal{T}(\mathbf{z})\rangle \right) \quad (9)$$

where $|\mathbf{z}\mathbf{z}'\rangle = \frac{1}{\sqrt{v}} \sum_{k=1}^{k=v} |\mathbf{k}\rangle_{\mathbf{z}} |\mathbf{k}\rangle_{\mathbf{z}'}$ is a maximally entangled state defined on any pair of legs connecting the nearby sites \mathbf{z} and \mathbf{z}' . These contractions connect all the legs into complete PEE threads (see Fig.3) and eventually we get the PEE tensor networks.

Factorized PEE tensor network— Let us consider a pair of PEE threads which makes a complete geodesic passing through \mathbf{z} , and we denote it as $C_{\mathbf{z}}(\mathbf{x}, \mathbf{x}') \equiv C_{\mathbf{z}}(\mathbf{x}) \cup C_{\mathbf{z}}(\mathbf{x}')$. Correspondingly we can divide the legs of \mathbf{z} into pairs and rewrite the quantum state (8) as,

$$|\mathcal{T}(\mathbf{z})\rangle = \mathcal{T}_{\mathbf{k}\mathbf{k}'}(\mathbf{z}) \left(\bigotimes_{C_{\mathbf{z}}(\mathbf{x}, \mathbf{x}')} |k_{\mathbf{x}}\rangle |k_{\mathbf{x}'}\rangle \right), \quad (10)$$

where \mathbf{k} (\mathbf{k}') denotes a collection of indices $\{k_{\mathbf{x}}\}$ ($\{k_{\mathbf{x}'}\}$). We define the factorized PEE tensor network in the following:

- Firstly, we set the tensor $\mathcal{T}_{\mathbf{k}\mathbf{k}'}(\mathbf{z})$ to be a tensor product of two-index tensors, each of which is associated to a pair of legs lying within the same complete PEE thread, such that the quantum state (8)

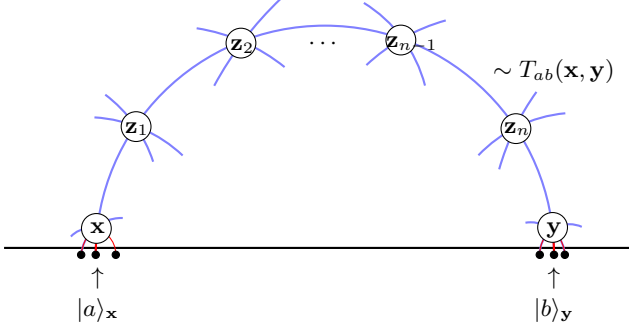


FIG. 3: Contraction of bulk tensors along a PEE thread results in a PEE thread with two open legs of the boundary sites tangent to the thread. In the factorized PEE tensor network, the thread represents a two-qudit state $T_{ab}(\mathbf{x}, \mathbf{y})|a\rangle_{\mathbf{x}}|b\rangle_{\mathbf{y}}$.

becomes a product of states associated to each pair of legs:

$$|\mathcal{T}(\mathbf{z})\rangle = \bigotimes_{\mathcal{C}_{\mathbf{z}}(\mathbf{x}, \mathbf{x}')} \mathcal{T}_{ab}(\mathbf{z})|k_{\mathbf{x}}\rangle|k_{\mathbf{x}'}\rangle. \quad (11)$$

- Furthermore, we require the state $\mathcal{T}_{ab}(\mathbf{z})|k_{\mathbf{x}}\rangle|k_{\mathbf{x}'}\rangle$ to be a pair of maximally entangled qudits, i.e. EPR pairs.

Then we contract all the internal legs to get the tensor network. Note that only the legs of adjacent sites are contracted along the PEE thread in between, hence the contractions are always along the PEE threads. More explicitly, let us consider a PEE thread $\mathcal{C}(\mathbf{x}, \mathbf{y})$ connecting boundary sites \mathbf{x} and \mathbf{y} , and write $\mathcal{C}(\mathbf{x}, \mathbf{y}) = \{\mathbf{x}, \mathbf{z}_1, \dots, \mathbf{z}_n, \mathbf{y}\}$ as a set of consecutive adjacent bulk sites with $n \rightarrow \infty$, we contract all the two-index tensors on $\mathcal{C}(\mathbf{x}, \mathbf{y})$ to get,

$$T_{ab}(\mathbf{x}, \mathbf{y}) \equiv \mathcal{T}_{ac_1}(\mathbf{x})\mathcal{T}_{c_1c_2}(\mathbf{z}_1)\dots\mathcal{T}_{c_nc_{n+1}}(\mathbf{z}_n)\mathcal{T}_{c_{n+1}b}(\mathbf{y}), \quad (12)$$

which is also a two-index tensor representing a pair of maximally entangled qudits. The contraction gives us a complete PEE thread with the two open legs tangent to $\mathcal{C}(\mathbf{x}, \mathbf{y})$ in the EPR state $|\psi\rangle_{\mathbf{xy}} = T_{ab}(\mathbf{x}, \mathbf{y})|a\rangle_{\mathbf{x}}|b\rangle_{\mathbf{y}}$, (see Fig.3). After the contraction along all the PEE threads, we get a tensor network representing the quantum state for all the boundary open legs:

$$|\Psi\rangle = \bigotimes_{\mathcal{C}(\mathbf{x}, \mathbf{y})} T_{ab}(\mathbf{x}, \mathbf{y})|a\rangle_{\mathbf{x}}|b\rangle_{\mathbf{y}}, \quad (13)$$

which is a product state of EPR pairs. The reduced density matrix for any one of the qudits in the EPR pairs satisfies:

$$\rho_{\mathbf{x}} = T_{ab}(\mathbf{x}, \mathbf{y})T_{cb}^*(\mathbf{x}, \mathbf{y})(|a\rangle\langle c|)_{\mathbf{x}} = \frac{\mathbb{1}_{\mathbf{x}}}{v}, \quad (14)$$

which demonstrates the unitarity of $T_{ab}(\mathbf{x}, \mathbf{y})$.

Now we consider any boundary region A in the state (13), and compute the entanglement entropy for A . It is convenient to classify all the PEE threads into three classes: (a) \mathcal{C}^A : threads that anchor only on A ; (b) $\mathcal{C}^{\bar{A}}$: threads that anchor only on \bar{A} ; (c) $\mathcal{C}^{A\bar{A}}$: threads that anchor on both A and \bar{A} at each end. Let us rewrite $|\Psi\rangle = |T^A\rangle \otimes |T^{\bar{A}}\rangle \otimes |T^{A\bar{A}}\rangle$ where

$$\begin{aligned} |T^A\rangle &\equiv \bigotimes_{\mathcal{C}(\mathbf{x}, \mathbf{y}) \in \mathcal{C}^A} T_{ab}^{(A)}(\mathbf{x}, \mathbf{y})|a\rangle_{\mathbf{x}}|b\rangle_{\mathbf{y}}, \\ |T^{\bar{A}}\rangle &\equiv \bigotimes_{\mathcal{C}(\mathbf{x}, \mathbf{y}) \in \mathcal{C}^{\bar{A}}} T_{ab}^{(\bar{A})}(\mathbf{x}, \mathbf{y})|a\rangle_{\mathbf{x}}|b\rangle_{\mathbf{y}}, \\ |T^{A\bar{A}}\rangle &\equiv \bigotimes_{\mathcal{C}(\mathbf{x}, \mathbf{y}) \in \mathcal{C}^{A\bar{A}}} T_{ab}^{(A\bar{A})}(\mathbf{x}, \mathbf{y})|a\rangle_{\mathbf{x}}|b\rangle_{\mathbf{y}}. \end{aligned} \quad (15)$$

Then we define pure states $\rho^{(A)} = |T^A\rangle\langle T^A|$, $\rho^{(\bar{A})} = |T^{\bar{A}}\rangle\langle T^{\bar{A}}|$, $\rho^{(A\bar{A})} = |T^{A\bar{A}}\rangle\langle T^{A\bar{A}}|$, and we have $\rho = |\Psi\rangle\langle \Psi| = \rho^{(A)} \otimes \rho^{(\bar{A})} \otimes \rho^{(A\bar{A})}$, which implies that

$$\rho_A = \text{Tr}_{\bar{A}} \rho = \rho_A^{(A)} \otimes \rho_A^{(\bar{A})} \otimes \rho_A^{(A\bar{A})}. \quad (16)$$

Note that $\rho_A^{(A)} = \rho^{(A)} = |T^A\rangle\langle T^A|$ is pure, and we also have $\rho_A^{(\bar{A})} = \langle T^{\bar{A}}|T^{\bar{A}}\rangle = 1$, hence $S(\rho_A^{(A)}) = S(\rho_A^{(\bar{A})}) = 0$. As for $\rho_A^{(A\bar{A})}$, according to the unitarity of $T_{ab}(\mathbf{x}, \mathbf{y})$ in (14), we have

$$\begin{aligned} \rho_A^{(A\bar{A})} &= \bigotimes_{\mathcal{C}(\mathbf{x}, \mathbf{y}) \in \mathcal{C}^{A\bar{A}}} (T(\mathbf{x}, \mathbf{y})T^{\dagger}(\mathbf{x}, \mathbf{y})) \\ &= \bigotimes_{\mathbf{x} \in A_1} \frac{\mathbb{1}_{\mathbf{x}}}{v} = \frac{\mathbb{1}_{A_1}}{v^{\mathcal{I}(A, \bar{A})}}, \end{aligned} \quad (17)$$

where A_1 denote the qudits in A that are connected to \bar{A} by the threads in $\mathcal{C}^{A\bar{A}}$, and $\mathcal{I}(A, \bar{A})$ counts the number of PEE threads in $\mathcal{C}^{A\bar{A}}$. Therefore, the entanglement entropy between A and \bar{A} is given by:

$$S_A = S(\rho_A^{(A\bar{A})}) = \mathcal{I}(A, \bar{A}), \quad (18)$$

where we have set $\log v = 1$ such that each thread gives unit contribution to S_A .

It has been demonstrated that [1], given a static boundary interval A (or any spherical region in higher dimensions) and the corresponding RT surface γ_A , the PEE threads in $\mathcal{C}^{A\bar{A}}$ are the only threads that intersect with γ_A , and each thread only intersects once. This means the number of intersections between γ_A and the PEE network is exactly $\mathcal{I}(A, \bar{A})$. Since the area of γ_A can be computed by counting the number of intersections (3), we have

$$S_A = \mathcal{I}(A, \bar{A}) = \frac{\text{Area}(\gamma_A)}{4G}, \quad (19)$$

which reproduces the RT formula for any static boundary single intervals and spherical regions. See the appendix

for more details for the bulk geometric picture, and another derivation for the RT formula by constructing isometric mappings from γ_A to the boundary.

Nevertheless, for disconnected and non-spherical connected boundary regions, the homologous surfaces Σ_A that only intersect with the threads in $\mathcal{C}^{A\bar{A}}$ no longer exists. Furthermore, the RT surface γ_A intersects not only with all the threads in $\mathcal{C}^{A\bar{A}}$, but also with a subset of the threads in \mathcal{C}^A or $\mathcal{C}^{\bar{A}}$ [1], which means $\mathcal{I}(A, \bar{A}) < \frac{\text{Area}(\gamma_A)}{4G}$. For these reasons we fail to reproduce the RT formula for generic boundary regions in this model.

Random PEE tensor network— In the second model, we also start from the PEE network, but set the states $|\mathcal{T}(\mathbf{z})\rangle$ (8) on the bulk vertices to be unit random states following [33]. We will take the random average of such states when computing the entropy quantities. To be specific, we take an arbitrary reference state $|0_{\mathbf{z}}\rangle$ and define $|\mathcal{T}(\mathbf{z})\rangle = U_{\mathbf{z}}|0_{\mathbf{z}}\rangle$ where $U_{\mathbf{z}}$ is a unitary operator, then the random average is equivalent to an integration over $U_{\mathbf{z}}$ according to the Haar probability measure. Again, after contracting all the internal legs of adjacent bulk sites along all the PEE threads using (9), we obtain the random PEE tensor network representing a boundary state for the boundary open legs.

In [33], the authors have shown that in a general graph of network with random tensors on the vertices, if we take the large v limit for the bond dimension of legs, the entanglement entropy for an arbitrary boundary region A is dominant by the area term:

$$S_A = \min \mathcal{N}(\Sigma_A) \log v, \quad (20)$$

where Σ_A is a surface in the network homologous to A , and $\mathcal{N}(\Sigma_A)$ counts the number of contracted tensor legs cut by Σ_A . Note that, the above result applies to general network graphs, including our PEE network. In this case, counting the minimal number of contracted legs cut by Σ_A is equivalent to computing the area of the minimal homologous surface γ_A , which is just the RT surface. Note that, in order to obtain the result (20), we need to set the contribution $\log v$ to the entropy from each thread to be a large number. Under this setup, we need to divide the density of the PEE threads by an overall constant $\log v$ to keep the boundary PEE unchanged. In other words, the density of intersections between any bulk surface and the PEE network becomes $1/(4G \log v)$, such that $\min \mathcal{N}(\Sigma_A) = \text{Area}(\gamma_A)/(4G \log v)$. Hence we reproduced the RT formula,

$$S_A = \min \mathcal{N}(\Sigma_A) \log v = \frac{\text{Area}(\gamma_A)}{4G} \quad (21)$$

We emphasize that the result in (20) applies to generic boundary regions, including disconnected and non-spherical connected regions.

Discussions— In this work, we assign quantum states to the vertices in the PEE network of AdS space and

build two PEE tensor network models, where the entanglement entropy can be explicitly computed. In our models, counting the minimal number of cuts in the tensor network is exactly computing the area of the RT surface in the semi-classical geometry of gravity. This provides the first example of taking natural continuous limit for a discrete tensor network to perfectly match the geometric background.

In the factorized model, the RT formula is only understood for spherical regions. This is not surprising as in this model all the PEE threads are decoupled from each other, which means the model is oversimplified for AdS/CFT. The factorized model reminds us of the bit thread configurations [67, 68], and we recommend the readers to consult [45] for their similarities and differences [69].

More interesting models can be developed by including coupling among the PEE threads. In the appendix, besides regarding the tensors as tensor product of two-index tensors, we also construct a HaPPY-like [46] PEE tensor network, where we associate a perfect tensor to each site in the PEE network. The RT formula for connected regions in AdS_3 is derived using a similar greedy algorithm developed in [46] for our HaPPY-like PEE tensor network.

As in [33, 46], we can also set open legs for the bulk sites to built a holographic code mapping the bulk states to the boundary states, then we can study the bulk quantum correction to the holographic entanglement entropy and identify the analogue of the quantum extremal surface [44]. Perhaps the most interesting future direction is to generalize the PEE tensor network to geometric background beyond the Poincaré AdS space, thus construct a new framework to study holographic correspondence beyond AdS/CFT. This is promising because the Crofton formula works for more generic Riemann manifolds, and we can build the network of all the geodesics in the Kinematic Space. The generalization will be non-trivial, as it is quite possible that the geodesics in the bulk will not always anchor on the boundary, which may correspond to spaces containing black holes or singularities.

Acknowledgments— The authors are supported by the NSFC Grant No. 12447108 and the Shing-Tung Yau Center of Southeast University. We thank Debarshi Basu for helpful discussions and related collaborations.

The RT formula in the factorized PEE tensor network

Before making a comparison between the factorized PEE tensor network with the HaPPY code [46], we first introduce some preliminary about isometric tensor for the section to be self-contained.

Definition 1. *An isometry from \mathcal{H}_A to \mathcal{H}_B is a linear map $T : \mathcal{H}_A \rightarrow \mathcal{H}_B$ with the property that it preserves*

the inner product (i.e. $\langle \psi | \phi \rangle = \langle T\psi | T\phi \rangle$, $\forall \psi, \phi \in \mathcal{H}_A$), such that

- $\dim(A) \leq \dim(B)$;
- $T^\dagger T = \mathbb{1}_A$, $TT^\dagger = \Pi_B$ where Π_B is a projector on $\text{Im}(V) \subset \mathcal{H}_B$.

Note that a unitary map is also an isometry, in the case that $\dim(A) = \dim(B)$. Given a complete orthonormal basis $\{|a\rangle\}$ for \mathcal{H}_A , and $\{|b\rangle\}$ for \mathcal{H}_B , we represent an isometry T as a two-index tensor:

$$T : |a\rangle \mapsto T_{ba}|b\rangle, \quad (22)$$

Then we have

$$T_{ba'}^* T_{ba} = T_{a'b}^\dagger T_{ba} = \delta_{a'a} \quad (23)$$

which we call an isometric tensor.

Proposition .2. *Given an isometry $T : |a_1 a_2\rangle \mapsto T_{ba_1 a_2}|b\rangle$ and if $\mathcal{H}_A = \mathcal{H}_{A_1} \otimes \mathcal{H}_{A_2}$, then there exists an isometry (up to a constant) $\tilde{T} : \mathcal{H}_{A_2} \rightarrow \mathcal{H}_B \otimes \mathcal{H}_{A_1}$ acting as*

$$\tilde{T} : |a_2\rangle \mapsto T_{ba_1 a_2} |ba_1\rangle \quad (24)$$

which obeys $\tilde{T}^\dagger \tilde{T} = \dim(A_1) I_{A_1}$.

Proof.

$$\begin{aligned} T_{ba'_1 a'_2}^* T_{ba_1 a_2} &= \delta_{a'_1 a'_2, a_1 a_2} = \delta_{a'_1 a_1} \delta_{a'_2 a_2} \\ \Rightarrow T_{ba_1 a'_2}^* T_{ba_1 a_2} &= \delta_{a_1 a_1} \delta_{a'_2 a_2} = \dim(A_1) \delta_{a'_1 a_1}. \end{aligned} \quad (25)$$

□

Proposition .3. *Given an isometry $T : |a\rangle \mapsto T_{ba}|b\rangle$ and, $\{|a\rangle\}$ and $\{|b\rangle\}$ form complete orthonormal bases for \mathcal{H}_A and \mathcal{H}_B respectively, then*

$$\{|T_a\rangle \equiv T|a\rangle = T_{ba}|b\rangle : 1 \leq a \leq \dim(A)\} \quad (26)$$

forms a set of orthonormal vectors for \mathcal{H}_B . Note that the index a ranges over $\dim(A)$ ($\leq \dim(B)$) values, so that (26) may not forms a basis for \mathcal{H}_B .

Proof.

$$\langle T_{a'} | T_a \rangle = \langle a' | T^\dagger T | a \rangle = \langle a' | \mathbb{1}_A | a \rangle = \delta_{a'a}. \quad (27)$$

□

Then let us look at the building blocks of our factorized PEE tensor network, which are the two-index tensors T_{ab} representing pairs of maximally entangled qudits. It implies that each tensor T_{ab} correspond to a unitary map from one leg to the other. Contracting these two-index tensors along PEE threads results in geodesic chords with two-index tensors representing unitary maps from the qudit in one of the endpoints to another. This includes

the two-index tensor $T(\mathbf{x}, \mathbf{y})$ in (14) for a complete PEE thread. More explicitly, (14) implies

$$T(\mathbf{x}, \mathbf{y}) T^\dagger(\mathbf{x}, \mathbf{y}) = \frac{\mathbb{1}_{\mathbf{x}}}{v}, \quad T^\dagger(\mathbf{x}, \mathbf{y}) T(\mathbf{x}, \mathbf{y}) = \frac{\mathbb{1}_{\mathbf{y}}}{v}, \quad (28)$$

hence $T(\mathbf{x}, \mathbf{y}) : |b\rangle_{\mathbf{y}} \mapsto T_{ab}(\mathbf{x}, \mathbf{y}) |a\rangle_{\mathbf{x}}$ is a unitary map between the pair of qudits shown in Fig.3 at the two boundary sites \mathbf{x} and \mathbf{y} . We can regard one leg of $T_{ab}(\mathbf{x}, \mathbf{y})$ as input while the other as output, hence define a unitary flow direction for all the threads, i.e. each PEE thread $\mathcal{C}(\mathbf{x}, \mathbf{y})$ has one incoming leg and one outgoing leg, giving a unitary map individually.

Now we consider any spherical boundary region A and, as in the main text, classify the PEE threads into three types: the \mathcal{C}^A , $\mathcal{C}^{\bar{A}}$ and $\mathcal{C}^{A\bar{A}}$, which are represented by the gray, orange and blue semi-circles in Fig.4a respectively for the special case of AdS_3 . Note that all the PEE threads are semi-circles and the RT surface γ_A of A is a semi-sphere, it is easy to observe that, all the PEE threads in \mathcal{C}^A and $\mathcal{C}^{\bar{A}}$ do not intersect with γ_A , while any thread in $\mathcal{C}^{A\bar{A}}$ intersects γ_A exactly once. Next we cut the AdS space open along the RT surface γ_A , giving open legs living on γ_A . All the legs on γ_A are all connected to a subset of the legs on A , which we call A_1 . It is convenient to divide the rest of the legs in A into two halves $A_2 \cup A_3$ such that the gray threads connect the legs in A_2 to those in A_3 . We further set the unitary flow direction for the threads $\mathcal{C}^{A\bar{A}}$ to be from the legs in γ_A to those in A_1 , and set the flow for the \mathcal{C}^A threads to be from A_2 to A_3 , then the threads in the entanglement wedge of A defines a unitary evolution from the legs in $\gamma_A \cup A_3$ to the legs $A_1 \cup A_2$. Similarly, we can divide the legs in \bar{A} into $\bar{A} = \bar{A}_1 \cup \bar{A}_2 \cup \bar{A}_3$, and set \bar{A}_1 to be the legs connected to γ_A , then the PEE threads defines a unitary evolution from the legs in $\bar{A}_1 \cup \bar{A}_2$ to those in $\gamma_A \cup \bar{A}_3$. The whole PEE tensor network is equivalent to a quantum circuit shown in Fig.4b.

It is easy to see that, the open legs $A_2 \cup A_3$ do not contribute to the entanglement entropy S_A , as they just correspond to a set of maximally entangled qudits which make a pure state. The only non-zero contribution to S_A comes from the legs A_1 , which are qudits maximally entangled to the legs \bar{A}_1 . If we set the entanglement contained in each thread to be one, then S_A is just given by the number of threads in $\mathcal{C}^{A\bar{A}}$, which equals to the number of intersections between γ_A and the PEE threads. Since the density of intersections on γ_A is $1/(4G)$ everywhere on γ_A , we reproduce the RT formula $S_A = \frac{\text{Area}(\gamma_A)}{4G}$.

It is also useful to derive the RT formula using the arguments in [46] for more generic tensor network models. To be specific, let us cut the tensor network open along a homologous surface \mathcal{C} whose boundary matches the boundary of A , such that the tensor network is divided into two parts \mathcal{P} and \mathcal{Q} , which are maps from \mathcal{C} to A and from \mathcal{C} to \bar{A} respectively. The boundary state can

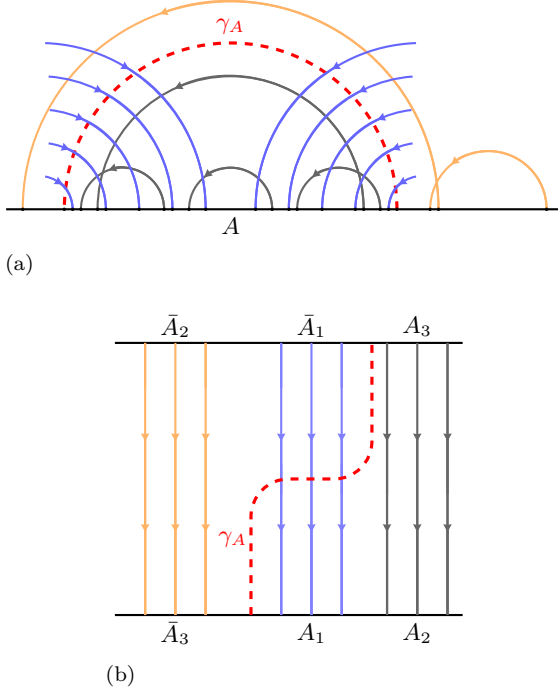


FIG. 4: (a) The three type of PEE threads, denoted by \mathcal{C}^A , $\mathcal{C}^{\bar{A}}$ and $\mathcal{C}^{A\bar{A}}$, are labeled by gray, orange and blue solid semi-circles respectively, while the RT surface γ_A is drawn as the red dashed line; (b) The circuit interpretation of the factorized PEE tensor network. Each PEE thread individually gives a unitary map, and the RT surface γ_A only cuts the threads in $\mathcal{C}^{A\bar{A}}$ once. The graph can be compared with Fig.19 of [46] where the ‘‘circuit’’ is built from the net effect of perfect tensors of certain bulk subregions as unitary gates.

be written as

$$|\Psi\rangle = \mathcal{P}_{\mathbf{a}\mathbf{c}}\mathcal{Q}_{\mathbf{b}\mathbf{c}}|\mathbf{a}\rangle_A|\mathbf{b}\rangle_{\bar{A}} = |\mathcal{P}_{\mathbf{c}}\rangle_A|\mathcal{Q}_{\mathbf{c}}\rangle_{\bar{A}}, \quad (29)$$

where $\{|\mathbf{a}\rangle\}$, $\{|\mathbf{b}\rangle\}$ runs over the complete bases for A and \bar{A} , and the index \mathbf{c} collects degrees of freedom associated to \mathcal{C} . Tracing \bar{A} we get the reduced density matrix,

$$\rho_A = \langle \mathcal{Q}_{\mathbf{c}'}|\mathcal{Q}_{\mathbf{c}}\rangle|\mathcal{P}_{\mathbf{c}}\rangle\langle\mathcal{P}_{\mathbf{c}'}|, \quad (30)$$

whose corresponding entanglement entropy S_A is upper bounded by the dimension of the Hilbert space on \mathcal{C} , i.e. the number of cuts $\mathcal{N}(\mathcal{C})$ between \mathcal{C} and the network. Then we get the minimal upper bound by choosing the homologous surface with minimal number of cuts, which we also denote as γ_A , hence

$$S_A \leq \mathcal{N}(\gamma_A) \log v. \quad (31)$$

Furthermore, according to the proposition (3), if the tensors \mathcal{P} and \mathcal{Q} are isometries, then $|\mathcal{Q}_{\mathbf{c}}\rangle$ and $|\mathcal{P}_{\mathbf{c}}\rangle$ are two sets of orthonormal vectors. This implies ρ_A is proportional to the identity such that the above inequality is saturated.

In the case of our factorized PEE tensor network model, we have:

- the homologous surface with minimal number of cuts is exactly the RT surface γ_A , and $\mathcal{N}(\gamma_A) = \text{Area}(\gamma_A)/4G$,
- by regarding $\{\gamma_A, A_3, A_1 \cup A_2\}$ as $\{a_2, a_1, b\}$ in the proposition 2, we can construct an isometry \mathcal{P} that maps γ_A to A , likewise we can construct an isometry \mathcal{Q} from γ_A to \bar{A} .

Therefore, the inequality is saturated and the RT formula follows upon setting $\log v = 1$.

HaPPY-like PEE tensor network

Besides regarding the tensors as tensor product of two-index tensors, we can also construct a HaPPY-like PEE tensor network, where we associate a perfect tensor on each site in the PEE network. Firstly, let us recall the definition of perfect tensor as follows:

Definition 4. A $2n$ -index tensor $T_{a_1 a_2 \dots a_{2n}}$ is a perfect tensor if, for any bipartition of its legs into a set D and complementary set D^c with $|D| \leq |D^c|$, T is proportional to an isometric tensor from D to D^c , where $|\cdot|$ denotes the number of legs in this set.

The definition implies that if we assign a flow configuration to a perfect tensor, the tensor always represents an isometric map as long as the number of incoming legs is less than or equal to the number of outgoing legs.

As was shown in [46], a bulk tensor network built from perfect tensors also satisfy the entropy bound (31), and the inequality is saturated if and only if the two tensors \mathcal{P} and \mathcal{Q} obtained by cutting the whole bulk tensor along γ_A are isometric. Since the graph of our network is the PEE network, again we have $\mathcal{N}(\gamma_A) = \text{Area}(\gamma_A)/4G$. In order to reproduce the RT formula, we only need to demonstrate that the mapping \mathcal{P} is an isometry that maps γ_A to A and \mathcal{Q} is an isometry that map γ_A to \bar{A} .

Now we build the isometric map from γ_A to A for our HaPPY-like PEE tensor network using an analogous greedy algorithm proposed in [46]. The procedure is decomposed into the following steps:

1. Given any connected boundary region A , let us consider a homologous surface Σ_A which cuts the PEE tensor network open, and we denote the region enclosed by A and Σ_A as \mathcal{W}_{Σ_A} (we do not include the sites on Σ_A into \mathcal{W}_{Σ_A}). In Fig.5, we mark \mathcal{W}_{Σ_A} as the blue region and Σ_A as the dashed red line. Note that, we require the tensor in \mathcal{W}_{Σ_A} to be an isometric map from the legs on Σ_A to those on A . More explicitly, here the legs on Σ_A means the legs emanating from Σ_A into the blue region.

2. Locally we consider any site on Σ_A and analyze whether the tensor on this site represents an isometry from the legs outside \mathcal{W}_{Σ_A} to those inside \mathcal{W}_{Σ_A} . In Fig.5, the black dashed line is the PEE thread tangent to Σ_A . Excluding the two legs on the dashed black thread, we find half of the legs stays inside \mathcal{W}_{Σ_A} , while the other half stays outside.
3. If the two dashed legs also stay in \mathcal{W}_{Σ_A} , then the number of legs in \mathcal{W}_{Σ_A} is greater than the number of outside legs (see Fig.5a), hence the perfect tensor on this site represents an isometric map from the outside legs to the inside legs. In this case we extend \mathcal{W}_{Σ_A} to swallow this site, hence the extended region still corresponds to a isometric map from the new Σ_A to A .
4. On the other hand, if the two dashed legs stay outside \mathcal{W}_{Σ_A} (see Fig.5c), then the tensor is not an isometric map from the outside legs to the inside legs, hence we should not absorb the site into \mathcal{W}_{Σ_A} .
5. Therefore, the critical configuration is that Σ_A locally matches the dashed geodesic (see Fig.5b).
6. Let us start from the Σ_A as the boundary interval A . Obviously it represents an isometry from the open legs to those stretch inside the AdS space. Then Σ_A moves into the bulk by swallowing more and more bulk sites, until each site of Σ_A matches the local critical configuration. This means the greedy algorithm halts when Σ_A matches the RT surface γ_A , such that we arrive at the least upper bound. Furthermore, the entanglement wedge \mathcal{W}_{γ_A} defines a isometric map from γ_A to A hence the upper bound (31) is saturated.

The advantage of our HaPPY-like PEE tensor network is that, the greedy algorithm is performed exactly in the AdS space instead of some discrete graph, and the minimal homologous surface exactly matches the RT surface. Nevertheless, as in the HaPPY code, the above arguments only works for connected regions and for a time slice of AdS_3 .

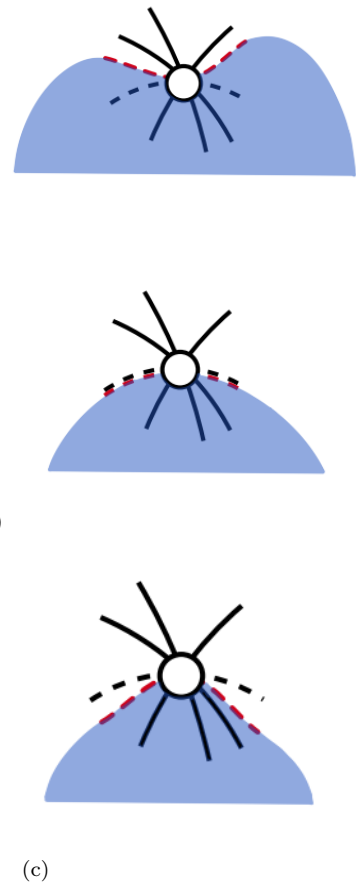


FIG. 5: Three local configurations for the legs emanating from one bulk site (the hollow circle) on the homologous surface Σ_A (red dashed line) in the PEE network. Here, \mathcal{W}_{Σ_A} is marked as the blue region, and the PEE thread tangent to Σ_A at this bulk site is marked as the black dashed line.

* Corresponding author: wenqiang@seu.edu.cn

† Co-first author: xumingshuai@seu.edu.cn

‡ Co-first author: zhonghaocheng@seu.edu.cn

[1] Jiong Lin, Yizhou Lu, Qiang Wen, and Yiwei Zhong. Weaving the (AdS) spaces with partial entanglement entropy threads. 1 2024.

- [2] Edward Witten. Anti-de Sitter space and holography. *Adv. Theor. Math. Phys.*, 2:253–291, 1998.
- [3] S. S. Gubser, Igor R. Klebanov, and Alexander M. Polyakov. Gauge theory correlators from noncritical string theory. *Phys. Lett. B*, 428:105–114, 1998.
- [4] Juan Martin Maldacena. The Large N limit of superconformal field theories and supergravity. *Adv. Theor. Math. Phys.*, 2:231–252, 1998.
- [5] Bartłomiej Czech, Joanna L. Karczmarek, Fernando Nogueira, and Mark Van Raamsdonk. The Gravity Dual of a Density Matrix. *Class. Quant. Grav.*, 29:155009, 2012.
- [6] Alex Hamilton, Daniel N. Kabat, Gilad Lifschytz, and David A. Lowe. Holographic representation of local bulk operators. *Phys. Rev. D*, 74:066009, 2006.
- [7] Ian A. Morrison. Boundary-to-bulk maps for AdS causal wedges and the Reeh-Schlieder property in holography. *JHEP*, 05:053, 2014.
- [8] Raphael Bousso, Stefan Leichenauer, and Vladimir Rosenhaus. Light-sheets and AdS/CFT. *Phys. Rev. D*, 86:046009, 2012.

[9] Raphael Bousso, Ben Freivogel, Stefan Leichenauer, Vladimir Rosenhaus, and Claire Zukowski. Null Geodesics, Local CFT Operators and AdS/CFT for Subregions. *Phys. Rev. D*, 88:064057, 2013.

[10] Veronika E. Hubeny and Mukund Rangamani. Causal Holographic Information. *JHEP*, 06:114, 2012.

[11] Aron C. Wall. Maximin Surfaces, and the Strong Subadditivity of the Covariant Holographic Entanglement Entropy. *Class. Quant. Grav.*, 31(22):225007, 2014.

[12] Matthew Headrick, Veronika E. Hubeny, Albion Lawrence, and Mukund Rangamani. Causality & holographic entanglement entropy. *JHEP*, 12:162, 2014.

[13] Daniel L. Jafferis, Aitor Lewkowycz, Juan Maldacena, and S. Josephine Suh. Relative entropy equals bulk relative entropy. *JHEP*, 06:004, 2016.

[14] Xi Dong, Daniel Harlow, and Aron C. Wall. Reconstruction of Bulk Operators within the Entanglement Wedge in Gauge-Gravity Duality. *Phys. Rev. Lett.*, 117(2):021601, 2016.

[15] Jordan Cotler, Patrick Hayden, Geoffrey Penington, Grant Salton, Brian Swingle, and Michael Walter. Entanglement Wedge Reconstruction via Universal Recovery Channels. *Phys. Rev. X*, 9(3):031011, 2019.

[16] Ahmed Almheiri, Xi Dong, and Daniel Harlow. Bulk locality and quantum error correction in AdS/CFT. *Journal of High Energy Physics*, 2015(4), apr 2015.

[17] Helia Kamal and Geoffrey Penington. The Ryu-Takayanagi Formula from Quantum Error Correction: An Algebraic Treatment of the Boundary CFT. 12 2019.

[18] Monica Jinwoo Kang and David K. Kolchmeyer. Entanglement wedge reconstruction of infinite-dimensional von Neumann algebras using tensor networks. *Phys. Rev. D*, 103(12):126018, 2021.

[19] Chris Akers and Geoff Penington. Quantum minimal surfaces from quantum error correction. *SciPost Phys.*, 12(5):157, 2022.

[20] Mingshuai Xu and Haocheng Zhong. Adding the algebraic Ryu-Takayanagi formula to the algebraic reconstruction theorem. 11 2024.

[21] Jason Crann and Monica Jinwoo Kang. Algebraic approach to spacetime bulk reconstruction. 11 2024.

[22] Brian Swingle. Entanglement Renormalization and Holography. *Phys. Rev. D*, 86:065007, 2012.

[23] Brian Swingle. Constructing holographic spacetimes using entanglement renormalization. 9 2012.

[24] Xiao-Liang Qi. Exact holographic mapping and emergent space-time geometry. 9 2013.

[25] Masamichi Miyaji, Tokiro Numasawa, Noburo Shiba, Tadashi Takayanagi, and Kento Watanabe. Continuous Multiscale Entanglement Renormalization Ansatz as Holographic Surface-State Correspondence. *Phys. Rev. Lett.*, 115(17):171602, 2015.

[26] Bartłomiej Czech, Lampros Lamprou, Samuel McCandlish, and James Sully. Tensor Networks from Kinematic Space. *JHEP*, 07:100, 2016.

[27] Daniel Harlow. The Ryu-Takayanagi Formula from Quantum Error Correction. *Commun. Math. Phys.*, 354(3):865–912, 2017.

[28] Romain Vasseur, Andrew C. Potter, Yi-Zhuang You, and Andreas W. W. Ludwig. Entanglement Transitions from Holographic Random Tensor Networks. *Phys. Rev. B*, 100(13):134203, 2019.

[29] Xi Dong, Daniel Harlow, and Donald Marolf. Flat entanglement spectra in fixed-area states of quantum gravity. *JHEP*, 10:240, 2019.

[30] Ling-Yan Hung, Wei Li, and Charles M. Melby-Thompson. p -adic CFT is a holographic tensor network. *JHEP*, 04:170, 2019.

[31] Ning Bao, Geoffrey Penington, Jonathan Sorce, and Aron C. Wall. Holographic Tensor Networks in Full AdS/CFT. 2 2019.

[32] see [24, 31, 33, 46, 48, 49, 70] for an incomplete list of recent progress.

[33] Patrick Hayden, Sepehr Nezami, Xiao-Liang Qi, Nathaniel Thomas, Michael Walter, and Zhao Yang. Holographic duality from random tensor networks. *JHEP*, 11:009, 2016.

[34] Jeevan Chandra and Thomas Hartman. Toward random tensor networks and holographic codes in CFT. *JHEP*, 05:109, 2023.

[35] Lin Chen, Ling-Yan Hung, Yikun Jiang, and Bing-Xin Lao. Deriving the non-perturbative gravitational dual of quantum Liouville theory from BCFT operator algebra. 3 2024.

[36] Ning Bao, Ling-Yan Hung, Yikun Jiang, and Zhihan Liu. QG from SymQRG: AdS₃/CFT₂ Correspondence as Topological Symmetry-Preserving Quantum RG Flow. 12 2024.

[37] Sami Kaya, Pratik Rath, and Kyle Ritchie. Hollowgrams: generalized entanglement wedges from the gravitational path integral. *JHEP*, 09:032, 2025.

[38] Sriram Akella. Tripartite entanglement in the HaPPY code is not holographic. 10 2025.

[39] Shinsei Ryu and Tadashi Takayanagi. Holographic derivation of entanglement entropy from AdS/CFT. *Phys. Rev. Lett.*, 96:181602, 2006.

[40] Veronika E. Hubeny, Mukund Rangamani, and Tadashi Takayanagi. A Covariant holographic entanglement entropy proposal. *JHEP*, 07:062, 2007.

[41] Horacio Casini, Marina Huerta, and Robert C. Myers. Towards a derivation of holographic entanglement entropy. *Journal of High Energy Physics*, 2011(5), may 2011.

[42] Aitor Lewkowycz and Juan Maldacena. Generalized gravitational entropy. *JHEP*, 08:090, 2013.

[43] Thomas Faulkner, Aitor Lewkowycz, and Juan Maldacena. Quantum corrections to holographic entanglement entropy. *JHEP*, 11:074, 2013.

[44] Netta Engelhardt and Aron C. Wall. Quantum Extremal Surfaces: Holographic Entanglement Entropy beyond the Classical Regime. *JHEP*, 01:073, 2015.

[45] Jiong Lin, Yizhou Lu, and Qiang Wen. Geometrizing the partial entanglement entropy: from PEE threads to bit threads. *JHEP*, 2024(02):191, 2024.

[46] Fernando Pastawski, Beni Yoshida, Daniel Harlow, and John Preskill. Holographic quantum error-correcting codes: Toy models for the bulk/boundary correspondence. *JHEP*, 06:149, 2015.

[47] Hewei Frederic Jia and Mukund Rangamani. Petz reconstruction in random tensor networks. *JHEP*, 10:050, 2020.

[48] Newton Cheng, Cécilia Lancien, Geoff Penington, Michael Walter, and Freek Witteveen. Random Tensor Networks with Non-trivial Links. *Annales Henri Poincaré*, 25(4):2107–2212, 2024.

[49] Xi Dong, Sean McBride, and Wayne W. Weng. Holographic tensor networks with bulk gauge symmetries. *JHEP*, 02:222, 2024.

[50] Qiang Wen. Fine structure in holographic entanglement and entanglement contour. *Phys. Rev. D*, 98(10):106004, 2018.

[51] Qiang Wen. Formulas for Partial Entanglement Entropy. *Phys. Rev. Res.*, 2(2):023170, 2020.

[52] Qiang Wen. Entanglement contour and modular flow from subset entanglement entropies. *JHEP*, 05:018, 2020.

[53] Muxin Han and Qiang Wen. Entanglement entropy from entanglement contour: higher dimensions. *SciPost Phys. Core*, 5:020, 2022.

[54] Muxin Han and Qiang Wen. First law and quantum correction for holographic entanglement contour. *SciPost Phys.*, 11(3):058, 2021.

[55] Jonah Kudler-Flam, Ian MacCormack, and Shinsei Ryu. Holographic entanglement contour, bit threads, and the entanglement tsunami. *J. Phys. A*, 52(32):325401, 2019.

[56] Guifre Vidal and Yangang Chen. Entanglement contour. *J. Stat. Mech.*, 2014(10):P10011, 2014.

[57] Qiang Wen. Towards the generalized gravitational entropy for spacetimes with non-Lorentz invariant duals. *JHEP*, 01:220, 2019.

[58] Debarshi Basu, Jiong Lin, Yizhou Lu, and Qiang Wen. Ownerless island and partial entanglement entropy in island phases. *SciPost Phys.*, 15(6):227, 2023.

[59] Andrew Rolph. Local measures of entanglement in black holes and CFTs. *SciPost Phys.*, 12(3):079, 2022.

[60] Yi-Yu Lin, Jia-Rui Sun, Yuan Sun, and Jie-Chen Jin. The PEE aspects of entanglement islands from bit threads. *JHEP*, 07:009, 2022.

[61] Yi-Yu Lin. Distilled density matrices of holographic partial entanglement entropy from thread-state correspondence. *Phys. Rev. D*, 108(10):106010, 2023.

[62] Qiang Wen. Balanced Partial Entanglement and the Entanglement Wedge Cross Section. *JHEP*, 04:301, 2021.

[63] Qiang Wen and Haocheng Zhong. Covariant entanglement wedge cross-section, balanced partial entanglement and gravitational anomalies. *SciPost Phys.*, 13(3):056, 2022.

[64] Qiang Wen, Mingshuai Xu, and Haocheng Zhong. Partial entanglement entropy threads in the island phase. *Phys. Rev. D*, 111(4):046027, 2025.

[65] Hugo A. Camargo, Pratik Nandy, Qiang Wen, and Haocheng Zhong. Balanced partial entanglement and mixed state correlations. *SciPost Phys.*, 12(4):137, 2022.

[66] Bartłomiej Czech, Lampros Lamprou, Samuel McCandlish, and James Sully. Integral Geometry and Holography. *JHEP*, 10:175, 2015.

[67] Michael Freedman and Matthew Headrick. Bit threads and holographic entanglement. *Commun. Math. Phys.*, 352(1):407–438, 2017.

[68] Matthew Headrick and Veronika E. Hubeny. Riemannian and Lorentzian flow-cut theorems. *Class. Quant. Grav.*, 35(10):10, 2018.

[69] In [45] it was demonstrated that bit threads configuration for spherical regions A can be reproduced by the superposition of the vector fields describing the PEE threads emanating from A .

[70] Zhao Yang, Patrick Hayden, and Xiao-Liang Qi. Bidirectional holographic codes and sub-AdS locality. *JHEP*, 01:175, 2016.